DEPARTMENT OF THE INTERIOR
UNITED STATES GEOLOGICAL SURVEY

Prepared for the
NATIONAL AERONAUTICS AND SPACE ADMINISTRATION

ATLAS OF MARS
1:5,000,000 GEOLOGIC SERIES
DIACRIA QUADRANGLE
M 5M 48/150 G, 1981
I-1286 (MC-2)

NOTES ON BASE

This map sheet is one of a series covering the entire surface of Mars at nominal scales of 1:25,000,000 and 1:5,000,000 (Batson, 1973; 1976). The major source of map data was the Mariner 9 television experiment (Masursky and others, 1970).

ADOPTED FIGURE

The figure of Mars used for the computation of the map projection is an oblate spheroid (flattening of 1/192) with an equatorial radius of 3393.4 km and a polar radius of 3375.7 km. This is not the height datum which is defined below under the heading "Contours".

PROJECTION

The Lambert conformal conic projection is used for this sheet with standard parallels at 35.8° and 59.2°. A scale of 1:4,336,000 at lat 30° was chosen to match the scale at lat 30° of the adjacent Mercator projections. Longitudes increase to the west in accordance with usage of the International Astronomical Union (IAU, 1971). Latitudes are areographic (de Vaucouleurs and others, 1973).

CONTROL

Planimetric control is provided by photogrammetric triangulation using Mariner 9 pictures (Davies, 1973; Davies and Arthur, 1973) and the radio-tracked position of the spacecraft. The first meridian passes through the crater Airy-O (lat 5.19° S) within the crater Airy. No simple statement is possible for the precision, but local consistency is about 10 km.

MAPPING TECHNIQUE

Selected Mariner 9 pictures were transformed to the Lambert conformal projection and assembled in a series of mosaics at 1:5,000,000.

CONTOURS

Because Mars has no seas and hence no sea level, the datum (the 0 km contour line) for altitudes is defined by a gravity field described by spherical harmonics of fourth order and fourth degree (Jordan and Lorell, 1973) combined with a 6.1-millibar atmospheric pressure surface derived from radio-occultation data (Kliore and others, 1973; Christensen, 1975; Wu, 1975, 1978).

The contour lines on most of the Mars maps (Wu, 1975, 1978) were compiled from Earth-based radar determinations (Downs and others, 1971; Pettengill and others, 1971) and measurements made by Mariner 9 instrumentation, including the ultraviolet spectrometer (Hord and others, 1974), infrared interferometer spectrometer (Conrath and others, 1973), and stereoscopic Mariner 9 television pictures (Wu and others, 1973).

Formal analysis of topographic elevation information has not been made. The estimated vertical accuracy of each source of data indicates a probable error of 1-2 km.

NOMENCLATURE

All names on this sheet are approved by the International Astronomical Union (IAU, 1974, 1977, 1980).

MC-2: Abbreviation for Mars Chart 2.
M 5M 48/150 G: Abbreviation for Mars 1:5,000,000 series; center of sheet, lat 48° N, long 150°; geologic map, G.

REFERENCES

Batson, R. M., 1973, Cartographic products from the Mariner 9 mission: Journal of Geophysical Research, v. 78, no. 20, p. 4424-4435.
______1976, Cartography of Mars: 1975: The American Cartographer, v. 3, no. 1, p. 57-63.
Christensen, E. J., 1975, Martian topography derived from occultation, radar, spectral, and optical measurements: Journal of Geophysical Research, v. 80, no. 20, p. 2909-2913.
Conrath, B. J., Curran, R. K., Hanel, R. A., Kunde, V. G., Maguire, W. W., Pearl, J. C., Pirraglia, J. A., Welker, J., and Burke, T. E., 1973, Atmospheric and surface properties of Mars obtained by infrared spectroscopy on Mariner 9: Journal of Geophysical Research, v. 78, no. 20, p. 4267-4278.
Davies, M. E., 1973, Mariner 9: Primary control net: Photogrammetric Engineering, v. 39, no. 12, p. 1297-1302.
Davies, M. E., and Arthur, D. W. G., 1973, Martian surface coordinates: Journal of Geophysical Research, v. 78, no. 20, p. 4355-4394.
Downs, G. S., Goldstein, R. M., Green, R. R., and Morris, G. A., 1971, Mars radar observations, a preliminary report: Science, v. 174, no. 4016, p. 1324-1327.
Hord, C. W., Simmons, K. E., and McLaughlin, L. K., 1974, Mariner 9 ultraviolet spectrometer experiment: Pressure-altitude measurements on Mars: Icarus, v. 21, no. 3, p. 292-302.
International Astronomical Union, Commission 16, 1971, Physical study of planets and satellites, *in* Proceedings 14th General Assembly, 1970: International Astronomical Union Transactions, v. 14B p. 128-137.
______1974, Physical study of planets and satellites, *in* Proceedings 15th General Assembly, 1973: International Astronomical Union Transactions, v. 15B, p. 105-108.
______1977, Physical study of planets and satellites, *in* Proceedings 16th General Assembly, 1976, International Astronomical Union Transactions, v. 16B, p. 325, 331-336, 355-362.
______1980, Physical study of planets and satellites *in* Proceedings 17th General Assembly, 1979: International Astronomical Union Transactions, v. 17B (in press).
Jordan, J. F., and Lorell, Jack, 1973, Mariner 9, an instrument of dynamical science: Presented at American Astronomical Society, American Institute of Aeronautics and Astronautics, Astrodynamics Conference, Vail, Colorado, July 16-18, 1973.
Kliore, A. J., Fjeldbo, Gunnar, Seidel, B. L., Sykes, M. J., and Woiceshyn, P. M., 1973, S-band radio occultation measurements of the atmosphere and topography of Mars with Mariner 9: Extended mission coverage of polar and intermediate latitudes: Journal of Geophysical Research, v. 78, no. 20, p. 4331-4351.
Masursky, Harold, Batson, R. M., Borgeson, W. T., Carr, M. H., McCauley, J. F., Milton, D. J., Wildey, R. L., Wilhelms, D. E., Murray, B. C., Horowitz, N. H., Leighton, R. B., Sharp, R. V., Thompson, T. W., Briggs, G. A., Chandeysson, P. L., Shipley, E. N., Sagan, Carl, Pollack, J. B., Lederberg, Joshua, Levinthal, E. C., Hartmann, W. K., McCord, T. B., Smith, B. A., Davies, M. E., de Vaucouleurs, G. D., and Leovy, C. B., 1970, Television experiment for Mariner Mars 1971: Icarus, v. 12, no. 1, p. 10-45.
Pettengill, G. H., Rogers, A. E. E., and Shapiro, I. I., 1971, Martian craters and a scarp as seen by radar: Science, v. 174, no. 4016, p. 1321-1324.
de Vaucouleurs, G. D., Davies, M. E., and Sturms, F. M., Jr., 1973, The Mariner 9 areographic coordinate system: Journal of Geophysical Research, v. 78, no. 20, p. 4395-4404.
Wu, S. S. C., 1975, Topographic mapping of Mars: U. S. Geological Survey Interagency Report 63, 191 p.
______1978, Mars synthetic topographic mapping: Icarus, v. 33, no. 3, p. 417-440.
Wu, S. S. C., Schafer, F. J., Nakata, G. M., Jordan, Raymond, and Blasius, K. R., 1973, Photogrammetric evaluation of Mariner 9 photography: Journal of Geophysical Research, v. 78, no. 20, p. 4405-4410.

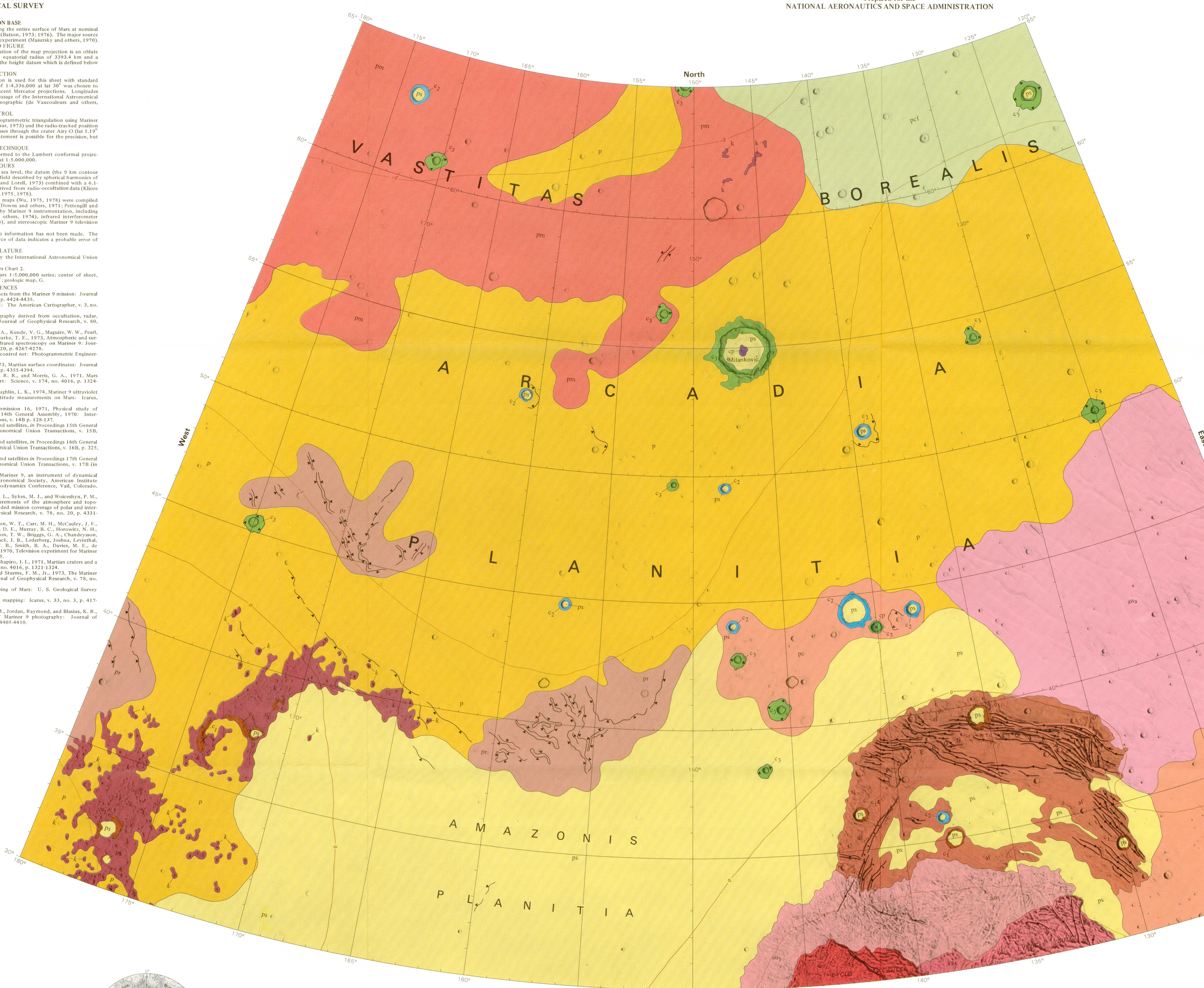

Interior—Geological Survey, Reston, Va—1981—G80301
Prepared on behalf of the Planetary Geology Program, Planetary Division, Office of Space Science, National Aeronautics and Space Administration under contract W-13, 709

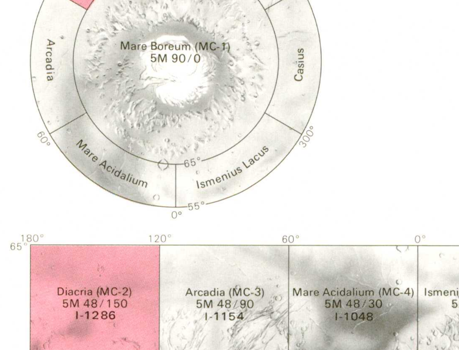

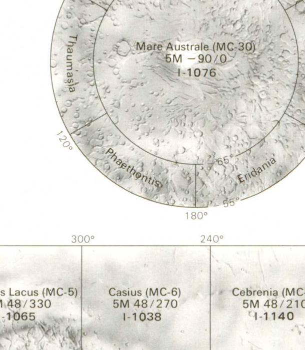

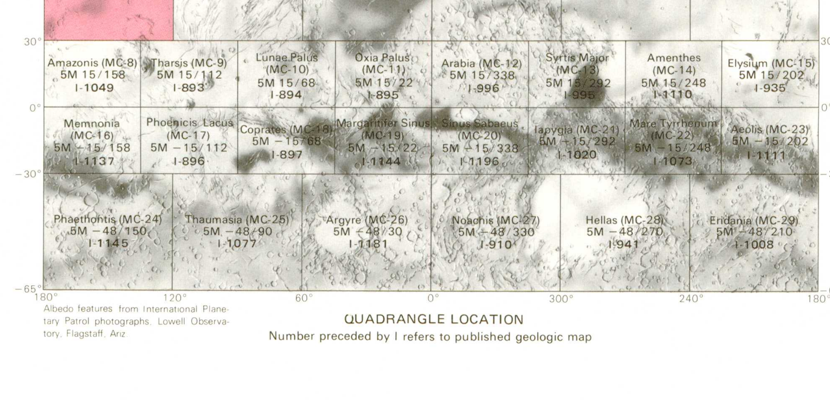

Albedo features from International Planetary Patrol photographs, Lowell Observatory, Flagstaff, Ariz.

QUADRANGLE LOCATION
Number preceded by I refers to published geologic map

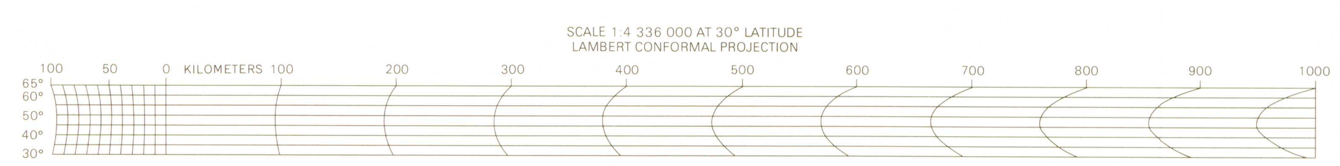

GEOLOGIC MAP OF THE DIACRIA QUADRANGLE OF MARS

By
E. C. Morris and K. A. Howard
1981

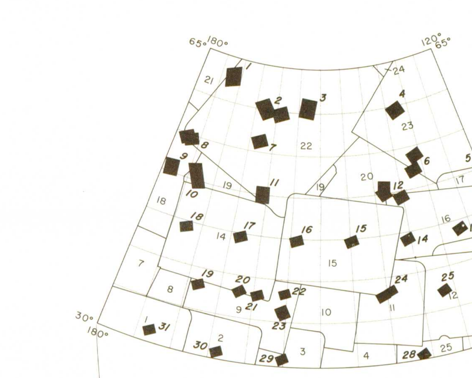

INDEX TO MARINER 9 PICTURES
The mosaic used to control the positioning of features on this map was made with the Mariner 9 A-camera pictures outlined above, identified by vertical numbers. Also shown (by solid black rectangles) are the high-resolution B-camera pictures, identified by italic numbers. The DAS numbers may differ slightly (usually by 5) among various versions of the same picture.

A-camera pictures

Index No.	DAS No.	Index No.	DAS No.
1	9342099	13	8298959
2	8011043	14	9342379
3	8082933	15	8083213
4	8154893	16	8227139
5	8298819	17	8299099
6	8370849	18	12327981
7	9270349	19	12328121
8	9342239	20	11481619
9	8011183	21	12152882
10	8083073	22	12328401
11	8155033	23	11482109
12	8226999	24	12502270
		25	8226859

High-resolution B-camera pictures

Index No.	DAS No.	Index No.	DAS No.
1	*7939188*	*15*	*8083248*
2	*6751988*	*16*	*8011358*
	8011638	*17*	*9342414*
3	*12328436*	*18*	*9270524*
4	*8227454*	*19*	*9342274*
5	*11481794*	*20*	*10615409*
6	*8155488*	*21*	*8011218*
	8227384	*22*	*6680028*
7	*8011568*	*23*	*9414024*
8	*9270734*		*9414164*
	9342624	*24*	*8155068*
9	*12328016*		*9557664*
10	*5276598*		*9557804*
11	*12328156*	*25*	*8227034*
12	*6895908*	*26*	*8298994*
	8155418	*27*	*8298854*
	11481654	*28*	*8226894*
13	*8227174*	*29*	*8082968*
14	*8155208*	*30*	*8011078*
		31	*9342134*

CORRELATION OF MAP UNITS

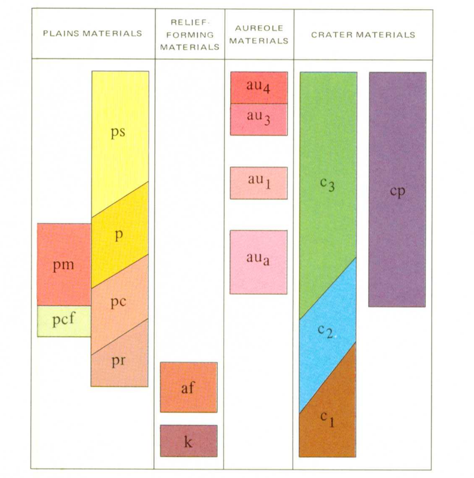

DESCRIPTION OF MAP UNITS

PLAINS MATERIALS

ps — SMOOTH PLAINS MATERIAL—Covers much of southern part of quadrangle. Flat, light, featureless surface at low resolution. Frequency of craters >1 km diameter 100 to $200/10^6 km^2$. *Interpretation:* Relatively thick volcanic and eolian deposits. Viking high-resolution pictures show a variety of materials from young fresh lava flows to thick eolian mantles that appear to display reticulate dune pattern. Extreme youth indicated by low crater population

p — PLAINS MATERIAL—Covers most of Arcadia Planitia in central part of quadrangle. Resembles smooth plains material but has greater crater population ranging from about 200 to $1000/10^6 km^2$ craters >1 km diameter. High-resolution Viking pictures show a greater variety of landforms than smooth plains unit, such as subdued hummocks and knobs, lobate flow structures, and pedestal craters. *Interpretation:* Volcanic and eolian deposits older than smooth plains material

pm — MOTTLED CRATERED PLAINS MATERIAL—Covers most of circumpolar plains of Mars. Has distinctive mottled appearance due to high-albedo material in and around craters that contrasts with darker plains material. Broad areas of hummocks and knobs and many pedestal and rampart craters. Interiors of most craters filled with high-albedo material. Moderately to highly cratered but small crater (< 10 km) population low. Mariner 9 pictures of very poor quality in this area. *Interpretation:* Highly eroded lava plains with eolian covering

pcf — CRATERED AND FRACTURED PLAINS MATERIAL—Similar to mottled cratered plains material but lacks conspicuous light-albedo material around craters; boundary between the two units drawn on the basis of albedo. Crater density similar to mottled cratered plains material. Has pedestal and rampart craters but lacks broad areas of hummocks and knobs. Subdued mantled appearance, interiors of small craters filled. *Interpretation:* Cratered lava plains blanketed by eolian deposits

pc — CRATERED PLAINS MATERIAL—Underlies southeastern part of quadrangle. Similar to plains material (unit p) but has greater small crater population and lacks hummocks, knobs, and pedestal craters. Has lobate scarps, ridges, and grabens trending northwest. Crater density range 2000 to 3500 craters >1 $km/10^6 km^2$. *Interpretation:* Lava plains similar to plains material (unit p) but older

pr — ROLLING PLAINS MATERIAL—Occurs in isolated areas within plains material unit; uneven surface, has distinctive etched texture with conspicuous curvilinear scarps, troughs, and depressions that trend generally northwest. *Interpretation:* Windows in plains material unit of older lava flows into which channels have been eroded by possible fluvial processes, thinly covered by eolian deposits

RELIEF-FORMING MATERIALS

af — ACHERON FOSSAE MATERIAL—Forms a semicircular deposit almost 700 km across; southern part is buried by aureole deposits of Olympus Mons. Surface is broken by grabens and extensive en echelon and parallel fractures and faults with varied displacements. Numerous small channels on crater walls, flanks of ridges, and in rough hummocky areas. Densely cratered (4000-5500 craters >1 $km/10^6 km^2$); most craters postdate fracturing. Central and southeastern parts form shallow basin filled with smooth plains material. *Interpretation:* Ancient low shield volcano that has been intensely eroded and fractured by recurring tectonic forces

k — KNOBBY MATERIAL—Consists of rounded to subangular, generally equi-dimensional hills forming rugged upland terrain. Forms part of rims and walls of craters older than c_2. High-resolution pictures show triangular faceted faces, conical forms, and elongate shapes that resemble terrestrial yardangs. Summit craters on conical forms rare. *Interpretation:* Remnants of ancient cratered terrain; dissected by faults and fractures and embayed by plains units

AUREOLE MATERIALS

OLYMPUS MONS AUREOLE MATERIALS—Occur as several overlapping sheets of distinctly textured and lineated terrain that form an asymmetric apron or aureole around Olympus Mons. They extend more than 1000 km northwest from center of Olympus Mons but only 600 km southeast. Four separate deposits have been recognized in adjacent Amazonis quadrangle (Morris and Dwornik, 1978). Only three of the aureole deposits are exposed in Diacria quadrangle. Each deposit can be distinguished from adjacent ones by length and width of ridges or their orientation. *Interpretation:* A series of overlapping pyroclastic deposits extruded prior to construction of Olympus Mons but associated with volcanism that produced the large shield volcano. Subsequent eolian erosion has modified surface forms of deposits

au_4 — AUREOLE DEPOSIT UNIT 4—Lies on and overlaps other Olympus Mons aureole deposits. Surface is characterized by a series of ridges and grooves that roughly parallel outer boundary of deposit. Individual ridge segments are 10 to 50 km long and form an anastomosing pattern that varies in length and width over different parts of deposit. Ridges are estimated to be as much as 1 km high. Their pattern is broken by several sets of intersecting, long, linear grooves that may be grabens or fractures with little displacement

au_3 — AUREOLE DEPOSIT UNIT 3—Partly covered by unit au_4 and rests upon unit au_1. At contact with unit au_4 ridges of unit au_4 trend generally N. 60° W., whereas ridges of unit au_3 trend about N. 20° E. Surface characteristics of unit au_3 are similar to those of unit au_4 in magnitude, and except for difference in trend of ridges at contact of two units, they are difficult to differentiate

au_1 — AUREOLE DEPOSIT UNIT 1—Oldest and most extensive of Olympus Mons aureole deposits. Surface features differ from overlying deposits mainly in size and are characterized by sets of anastomosing ridges and alined hills and knobs as much as 10 km long; these features are in some parts alined roughly with outer edge of deposit but in other areas at right angles to edge. Where well exposed, ridges are closely spaced (approximately 30 to 40 ridges per 100-km distance). High-resolution pictures (DAS-8226894) of ridges show aerodynamic shapes similar in form to terrestrial yardangs

au_a — ALBA PATERA AUREOLE MATERIAL—Around Alba Patera to the east, forms part of a concentric ring of radial flow channels, anastomosing low elongate ridges, flow lobes, and elongate fingerlike structures. Locally some faults, chain craters, and grabens. Crater density range 1500-2300 craters >1 $km/10^6 km^2$. *Interpretation:* Low-viscosity, probably basaltic lava flows that make up distal parts of large volcanic shield of Alba Patera

CRATER MATERIALS

Craters are classified according to relative age on the basis of their morphologic characteristics. Craters less than 20 km diameter were not mapped. Most craters in the following categories are believed to be of impact origin.

c_3 — MATERIALS OF RIMMED CRATERS—Rims complete, raised, and rough appearing where diameter is >30 km. Floors lower than adjacent terrain; rough in craters >30 km, craters <30 km bowl-shaped, central peaks common and conspicuous

c_2 — MATERIAL OF SUBDUED CRATERS—Rims similar to c_3 craters but generally have narrow, smooth walls. Floors smooth, flat, lower than adjacent terrain. Central peaks small or absent

c_1 — MATERIAL OF HIGHLY DEGRADED CRATERS—Rims incomplete; consist in large part of knobby material. Floors like those of c_2 craters but about same elevation as adjacent terrain. Central peaks absent

cp — CENTRAL PEAK MATERIAL—Forms prominent hills near centers of c_3 age craters. *Interpretation:* Brecciated crater floor uplifted by rebound during shock decompression following compressive stage of impact

Contact

Fault scarp—Bar and ball on low side. On narrow grabens ball is centered between lines or is on single line representing both faults

Scarp—Line at base, barb points downslope. *Interpretation:* Flow front, fault scarp, or erosional scarp bounding pedestal crater

Crater rim crest—Not shown around smaller craters or where indistinct

INTRODUCTION

The Diacria quadrangle lies within the north circumpolar lowlands of Mars (Carr and others, 1973; Scott and Carr, 1978). The dominant structural and physiographic features are low, relatively smooth plains (Arcadia Planitia, Vastitas Borealis) that form the northern two-thirds of the quadrangle. The plains rise to the south to form the north edge of the Amazonis Planitia and to the southeast toward two major volcanic provinces of Mars, Olympus Mons and Alba Patera. The aureole deposits of these large volcanoes dominate the terrain of the southeastern part of the quadrangle. An area of rough knobby terrain occurs in the southwestern part of the quadrangle and rises toward the Elysium volcanic province that lies 1600 km to the west.

Original mapping of this quadrangle was from Mariner 9 pictures. The mapping was revised after high-resolution Viking Orbiter pictures were acquired. The Viking pictures, where available, were used to determine crater statistics and the nature and detail of stratigraphic units. Many Mariner 9 pictures were of poor quality because of haze and cloud layers over most of the quadrangle, particularly the north half. Many Viking pictures also contained haze and clouds in these areas.

GEOLOGIC SUMMARY

The oldest rock exposed in the Diacria quadrangle is rough knobby material in the southwest where the central plains rise toward Elysium Mons (DAS-09342099). This is the knobby material of Scott and Carr (1978); it was included in the knobby terrain unit of McCauley and others (1972) and the fretted terrain unit of Sharp (1973). The knobby material is overlapped and buried by plains units. Most exposures of knobby material are in the plains units and form islandlike knobs rising above the level plains. Much of the knobby material is arranged in vague arcuate and circular outlines suggestive of old eroded craters. The absence of recognizable c_1 or c_2 craters with coherent rims within knobby material suggests that the knobby material has had an intense erosional history that has mostly destroyed the older craters. The knobby material probably is composed mostly of impact breccias.

The next oldest unit is the Acheron Fossae material, a semicircular deposit almost 700 km across near the southeast corner of the quadrangle (DAS-08227039, Viking 129A36). Plains material laps up on and covers the outer edges of the deposit and fills a shallow basin in its central and southeastern parts. The southern part is buried beneath the aureole deposits of Olympus Mons. The surface is broken by an extensive system of parallel grabens and en echelon faults (Acheron Fossae) that generally trend northwestward (N. 50° - 70° W.). High-resolution Viking pictures show the fracturing and faulting to be most intense along the east edge of the deposit where numerous sliverlike fault blocks show different amounts of displacement (Viking 040B30). The unit is heavily cratered, but most cratering postdates faulting, evidence indicating an old age for the episode of faulting. In high-resolution pictures, many areas of the Acheron Fossae material have numerous small dendritic channels on crater walls and flanks of ridges and in rough hummocky areas (Viking 130A29). The arcuate form of the deposit and its location near Olympus Mons suggest that the Acheron Fossae material may be the remnant of an old volcano, similar to Alba Patera, that was ancestral to Olympus Mons and its aureole deposits.

Plains-forming material dominates the quadrangle; its age extends over much of the decipherable history of this part of Mars. The oldest plains unit is rolling plains material, exposed as patches or windows in the younger overlying plains material. The rolling plains material is characterized by low, rolling, elongate highs, indistinct lows, prominent curvilinear scarps, and troughs and depressions trending generally northwest. High-resolution Viking pictures show that the surface of some exposures of rolling plains material has an etched appearance similar to that of terrestrial thermokarst terrain, but with a mantle of eolian material that buries and subdues it (Soderblom and others, 1973). The undulatory character of the rolling plains, and the ridges, scarps, and troughs, suggest that the material is mostly volcanic plains formed by lavas, probably basalts, into which channels have been eroded by possible fluvial processes. The eroded lavas subsequently may have been blanketed by a thin covering of eolian deposits.

The cratered plains material is at least partly equivalent in age to the cratered and fractured plains material and the mottled cratered plains material. The cratered plains material is exposed in the southeastern part of the quadrangle; the other two units form part of the circumpolar plains and cover the northern third of the quadrangle. Crater densities appear to be similar for all three units, particularly for craters > 20 km, but determinations are less reliable for the northern plains because of poor picture quality. Small craters < 10 km are more abundant and better preserved on the cratered plains unit, possibly because more active erosional and depositional processes in the northern plains have resurfaced the area, obliterating the smaller craters (Soderblom and others, 1973). The mottled cratered plains material and the cratered and fractured plains material have abundant pedestal and rampart craters; the interiors of most small craters are filled. The cratered plains unit has no pedestal craters, and the interiors of the more abundant small craters are not filled.

The most distinctive characteristic of the mottled cratered plains material is the mottling caused by a strong albedo contrast between bright material around the larger craters and darker plains material in the intercrater areas. In high-resolution Viking pictures, the intercrater areas are covered with conical to elongate knobs 2-4 km across and broad, less distinct hummocks 4-8 km across. The knobs and hummocks have a subdued appearance owing to a mantling of eolian material (Soderblom and others, 1973).

Plains and smooth plains materials are the youngest materials exposed in the Diacria quadrangle and cover over half its area. They lap up on and partially bury all other units and fill interiors of large craters. The distinction between plains and smooth plains is based mainly upon a slightly greater crater population for the plains material, particularly craters >10 km. The Viking pictures reveal considerably diversity of materials and landforms that make up both smooth plains and plains materials. Both units show landforms that are indicative of both volcanic and eolian materials. Sequences of low, lobate scarps extend over broad areas and most likely are the termini of lava flows. The scarps and surfaces of some flows are rough appearing and are sculpted, probably by eolian action, into parallel linear forms, grooves, and ridges, similar to terrestrial yardangs (McCauley, 1973). Other areas are shown in the Mariner pictures as broad, featureless terrain but in the Viking pictures have a pattern of fine parallel or reticulate ridges that are interpreted as dunes. In the highest resolution Viking pictures, the dunes appear to be almost ubiquitous on the plains and smooth plains units. Viking pictures also show the plains unit to have abundant small pedestal craters, rampart craters (McCauley, 1973), and small knobs and hummocks. These features appear to be less prominent on the smooth plains material. Interiors of the small craters on the plains material unit appear to be filled, but the mantling of eolian material is not so thick as on the mottled cratered and the cratered and fractured plains units to the north. On the smooth plains unit, only a few small craters have filled interiors.

The smooth plains material probably contains some of the youngest lava flows exposed on the planet. A sequence of very young flows in the southeastern part of the quadrangle extends around the east edge of the aureole deposits of Olympus Mons and buries part of the cratered plains and Acheron Fossae materials. The population of craters >1 km is less than $328/10^6 km^2$ on those flows (Schaber and others, 1978).

Aureole deposits, because of their spatial arrangement surrounding Olympus Mons and Alba Patera (Morris and Dwornik, 1978; Wise, 1979), are clearly associated with the volcanism that produced these large shield volcanoes. The Alba Patera aureole is, in effect, the flank deposit of this huge, broad, low shield volcano. The deposit consists of long lava flow channels, anastomosing low elongate ridges, flow lobes, and long fingerlike flows, all radial to the central caldera of Alba Patera (Wise, 1979). Several northwest-trending faults and chains of craters break the radial pattern of flows and lava channels. The crater population on the Alba Patera aureole ($1500\text{-}2300/10^6 km^2$) indicates an age slightly younger than that of the cratered plains that are buried by the aureole deposits in the southeastern part of the quadrangle.

The aureole deposits of Olympus Mons, also referred to as grooved terrain (McCauley and others, 1972), occur as several overlapping sheets of distinctly textured and lineated terrain that are asymmetric to the large shield volcano. These sheets extend almost 1000 km northwest from the center of Olympus Mons but only 600 km southeast. These deposits differ distinctly from the aureole deposits of other volcanic shields on Mars. The Olympus Mons aureole material lacks the flow lobes, lava channels, radial ridges, and long fingerlike flows that are characteristic of the other aureole deposits (Wise, 1979). The surfaces of the Olympus Mons deposits are characterized by an anastomosing pattern of ridges and grooves that vary in length, width, and spacing over different parts of the deposits. In some deposits the ridges mostly parallel the outer boundary of the deposit, whereas in other deposits they are randomly oriented or perpendicular to the boundary of the deposit. Each aureole deposit can be distinguished from adjacent ones by the length, width, and orientation of the ridges. From shadow measurements, the ridges are estimated to be as much as 1 km high, and individual segments range in length from 10 to 50 km. Those that parallel the margins of the deposits are interpreted to be pressure ridges formed on viscous material normal to the direction of flow during emplacement. The pattern of the ridges is broken by sets of intersecting, long, linear grooves that may be grabens or fractures with little displacement. The fractures are restricted to individual units and do not cross unit boundaries.

The Olympus Mons aureole deposits are believed to be ash flows from huge pyroclastic eruptions that occurred at various times prior to the construction of Olympus Mons. There were at least four and possibly six eruptions; the oldest and largest extruded more than $2.5 \times 10^6 km^3$ of pyroclastic material —unit au_1 (Morris, 1980).

The oldest deposit (unit au_1) was extensively eroded before being partly buried by the younger deposits. The primary ridge structures that were parallel to the margins in many parts of the oldest unit were modified, possibly by eolian processes, into a secondary set of ridges nearly normal to the trend of the primary ridges. In some areas the secondary set of erosional ridges has almost completely obliterated the primary ridge structure (Viking 851A29). Little modification of the ridges on the younger deposits indicates a lapse of time between the eruption of the oldest unit and the emplacement of younger aureole deposits.

The easy erodibility of the soft ash flow deposits is indicated by the modification of primary ridge structures and also by the rapid destruction of impact craters on the aureole deposits. There are only 43 craters $\gtrsim$1 km on the total $8.3 \times 10^5 km^2$ exposed area of the aureole deposits ($53 \times 10^6 km^2$). The plains material that buried the margins of the aureole has a greater crater population than the aureole (Schaber and others, 1978).

The fractures and grabens that cut the ridges and grooves are probably contraction cracks formed during the cooling of the huge ash flows.

GEOLOGIC HISTORY

The geologic history of the Diacria quadrangle, interpreted from stratigraphic relations of the mapped rock units, began with erosion of ancient cratered terrain to form the knobby material. This material probably represents remnants of densely cratered and hilly terrain that developed early in the history of Mars during a period of intense meteorite bombardment. After the decline of the high impact flux, there was a long period of erosion and degradation of the cratered terrain, with subsequent development of the knobby terrain (Scott and Carr, 1978). Many of the rim deposits of the old craters survive only as vague circular arrangements of knobs. A large low shield volcano in the area of the Acheron Fossae developed during the waning stages of this period of erosion and degradation and prior to the great outpouring of lavas that formed the northern plains of Mars. The central area of the shield volcano subsided and the structure was highly fractured during a period of intense faulting associated with broad updoming in the Tharsis region (Carr, 1975) to the southeast.

The next major event was the flooding of the old cratered and knobby terrain in the central and southern regions of the map area by a thick series of basalts that formed the rolling plains material. The undulatory character of this unit and some of its ridges and scarps may reflect the buried topography of the old cratered plains.

The emplacement of the rolling plains material was followed by a period of intense eolian activity during which the rolling plains and knobby material were eroded and buried in places under a blanket of eolian debris. Periods of volcanic outpourings and eolian deposition and erosion continued, forming the various plains units that now cover most of the quadrangle. The incorporation into the eolian deposits of volatiles frozen out of the atmosphere in the northern circumpolar plains region probably is responsible for the appearance of the mottled cratered plains material. The abundance of rampart craters in the northern plains suggests that these sediments may contain more ground ice than the southern plains units (Johansen, 1979). Also, eolian erosion and deposition were more intense in the northern plains than in the southeastern part of the quadrangle: pedestal craters are common in the mottled cratered and the cratered and fractured plains material of the north but are absent in the cratered plains material of the southeast.

Partly contemporaneous with the formation of the cratered plains, cratered and fractured plains, and mottled cratered plains units, a large shield volcano, Alba Patera, developed east of the Diacria area. Lavas from this broad shield volcano flowed westward down its flank into Arcadia Planitia and formed part of the Alba Patera aureole in the southeastern part of the quadrangle. The lavas buried parts of the Acheron Fossae material and the cratered plains material.

After formation of the plains materials and Alba Patera, a different type of volcanic activity commenced in the vicinity of Olympus Mons (Morris, 1980). A great pyroclastic eruption poured out more than 1 million km^3 of ash flow tuffs. This huge deposit of pyroclastic material, over 1800 km in diameter and probably a kilometer thick, buried the south half of the Acheron Fossae material and parts of the cratered plains material. This eruption was followed by a period of intense erosion of the soft pyroclastic materials. Surface features were eroded into streamlined forms that paralleled the prevailing winds. After this period of erosion, more eruptions at several localities formed other Olympus Mons aureole deposits. Olympus Mons subsequently grew to its enormous size by later effusive eruptions.

The final episode shaping the surface in the Diacria quadrangle was the eruption of a sequence of lava flows that covered parts of Amazonis Planitia. Very young lava flows of this episode flowed from the Tharsis region northward, filling a circumferential basin around Olympus Mons and covering parts of the cratered plains. Eolian deposits filled the interiors of many craters and blanketed the basin south of Acheron Fossae.

REFERENCES

Carr, M. H., 1975, Geologic map of the Tharsis quadrangle of Mars: U.S. Geological Survey Miscellaneous Geologic Investigations Map I-893.
Carr, M. H., Masursky, Harold, and Saunders, R. S., 1973, A generalized geologic map of Mars: Journal of Geophysical Research, v. 78, p. 4031-4036.
Johansen, L. A., 1979, Martian splosh cratering and its relation to water: *in* Second International Colloquium of Mars, NASA Conference Publication 2082, p.44.
McCauley, J. F., 1973, Mariner 9 evidence for wind erosion in the equatorial and mid-latitude regions of Mars: Journal of Geophysical Research, v. 78, p. 4123-4137.
McCauley, J. F., Carr, M. H., Cutts, J. A., Hartmann, W. K., Masursky, Harold, Milton, D. J., Sharp, R. P., and Wilhelms, D. E., 1972, Preliminary Mariner 9 report on the geology of Mars: Icarus, v. 17, p. 289-327.
Morris, E. C., 1980, A pyroclastic origin for the aureole deposits of, Olympus Mons: Reports of Planetary Geology Program, 1980, NASA Technical Memorandum 82385, p. 252-254.
Morris, E. C., and Dwornik, S. E., 1978, Geologic map of the Amazonis quadrangle of Mars: U.S. Geological Survey Miscellaneous Geologic Investigations Map I-1049.
Schaber, G. G., Horstman, K. C., and Dial, A. L., Jr., 1978, Lava flow materials in the Tharsis region of Mars: Proceedings Lunar and Planetary Science Conference, 9th, Houston, Texas, p. 3433-3458.
Scott, D. H., and Carr, M. H., 1978, Geologic map of Mars: U.S. Geological Survey Miscellaneous Geologic Investigations Map I-1083.
Sharp, R. P., 1973, Mars: Fretted and chaotic terrains: Journal of Geophysical Research, v. 78, p. 4073-4083.
Soderblom, L. A., Kreidler, T. J., and Masursky, Harold, 1973, Latitudinal distribution of a debris mantle on the martian surface: Journal of Geophysical Research, v. 78, p. 4117-4122.
Wise, D. E., 1979, Geologic map of the Arcadia quadrangle of Mars: U.S. Geological Survey Miscellaneous Geologic Investigations Map I-1154.

For sale by Branch of Distribution, U.S. Geological Survey, 1200 South Eads Street, Arlington, VA 22202, and Branch of Distribution, U.S. Geological Survey, Box 25286, Federal Center, Denver, CO 80225